ratio of $m_e/m_{lh}\simeq 0.7$ is obtained which is reasonable for electrons and light holes. This value is somewhat larger than the ratio $m_e/m_{lh}\simeq 0.58$ calculated from the values listed by Cardona.[11]

The author wishes to thank Dr. H. C. Casey, Dr. P. K. Tien, Dr. S. J. Buchsbaum, and Dr. P. J. Dean for helpful comments on the manuscript. He also thanks Dr. J. W. Gray for several useful discussions.

PHYSICAL REVIEW VOLUME 178, NUMBER 3 15 FEBRUARY 1969

Optical Third-Order Mixing in GaAs, Ge, Si, and InAs*

J. J. WYNNE
Gordon McKay Laboratory, Division of Engineering and Applied Physics, Harvard University, Cambridge, Massachusetts 02138

(Received 19 August 1968)

Nonlinear optical difference mixing of CO_2 laser radiation is studied in the semiconductors GaAs, Ge, Si, and InAs. The fourth-rank electric susceptibility tensor receives independent contributions from the bound or valence electrons, χ^b, and, in n-type material, from the conduction electrons, χ^n. These two contributions are separated and measured in GaAs. χ^b is found to be anisotropic and χ^n to be isotropic for carrier concentrations $n\leqslant 5\times 10^{16}$/cc. The relative signs of the susceptibilities are determined. χ^b in Ge and GaAs and χ^n in GaAs and InAs all have the same sign for the particular frequency combination studied. Theoretical and experimental evidence indicate that this sign is positive. At room temperature, χ^n in GaAs is a linear function of n for $n\leqslant 5\times 10^{16}$/cc. The value of the slope $\partial\chi^n/\partial n$ is a direct measure of the nonparabolicity of the conduction band in GaAs. It is shown to be inconsistent with Kane's model for small direct-band-gap semiconductors, and in agreement with Cardona's indirect measurements of the nonparabolicity in GaAs.

I. INTRODUCTION

THE existence of a nonvanishing electric polarization cubic in electric field strength offers the possibility of studying optical nonlinearities in centrosymmetric crystals. In noncentrosymmetric crystals the effects of a polarization cubic in the field are usually much smaller than quadratic polarization effects, but the cubic effects may be singled out for study. Several workers have studied polarizations third order in electric field. Maker and Terhune[1] studied materials transparent in the visible using a pulsed ruby laser. More recently, the CO_2 laser has been used[2–4] to study semiconductors which are not transparent in the visible.

Jha and Bloembergen[5] (JB) have shown that, for n-type semiconductors of group IV and the III-V type, the nonlinear susceptibility may be separated into two independent contributions, the bound or valence electron contribution χ^b and the conduction-electron contribution χ^n. Wynne and Boyd[4] (WB) measured the effect of the valence electrons χ^b in Ge and Si, and JB calculated χ^b for Ge, Si, GaAs, InAs, InSb, and GaSb using stationary state perturbation theory to derive nonlinear susceptibilities in terms of multipole moments in a tetrahedral-bonding orbital ground state. The agreement in magnitude to within the experimental error is encouraging, but, as shall be seen, there are still serious discrepancies.

Wolff and Pearson[6] (WP) made a simple one-band calculation of the conduction-electron contribution χ^n based on Kane's[7] band structure for InSb. Their results are in good agreement with the experimental results of Patel, Slusher, and Fleury[2] for InAs and InSb. JB have shown that the WP results for χ^n need a correction when the photon energies are not very small compared to the energy gap between conduction and valence bands.

The experimental work has been extended to measure both χ^b and χ^n in GaAs for varying carrier concentration. In addition the anisotropy and the relative signs of χ^b and χ^n have been determined in Ge, GaAs, and InAs ($n\approx 2.6\times 10^{16}$/cc) using an interference technique. In Sec. II, the experimental method of determining χ is discussed. All measurements were made relative to the absolute determination of χ in Ge by WB. The basic experimental uncertainty of $\pm 50\%$ in the magnitude of χ(Ge) carries over to all measured χ, but the relative measurements are more accurate. In Sec. III, the experimental results are presented and compared with theory in terms of magnitude and sign.

* This research was supported in part by the Advanced Research Projects Agency under contract No. SD-88 and in part by the U. S. Joint Services under contract N00014-67-A-0298-0006.

[1] P. D. Maker and R. W. Terhune, Phys. Rev. 137, A801 (1965).
[2] C. K. N. Patel, R. F. Slusher, and P. A. Fleury, Phys. Rev. Letters, 17, 1011 (1966).
[3] J. H. McFee, Appl. Phys. Letters 11, 228, (1967).
[4] J. J. Wynne and G. D. Boyd, Appl. Phys. Letters 12, 191, (1968).
[5] S. S. Jha and N. Bloembergen, Phys. Rev. 171, 891 (1968).
[6] P. A. Wolff and Gary A. Pearson, Phys. Rev. Letters 17, 1015 (1966).
[7] E. O. Kane, J. Phys. Chem. Solids 1, 249 (1957).

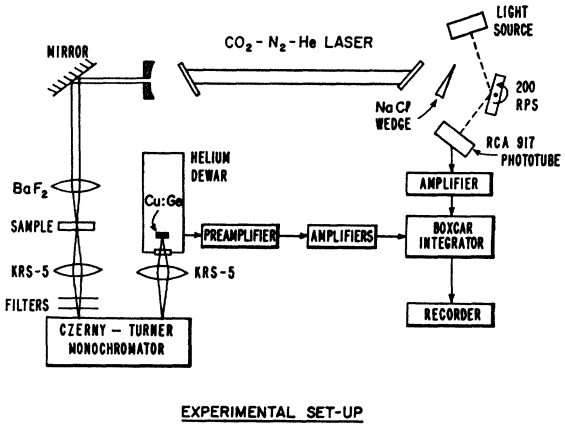

FIG. 1. Schematic diagram for detecting and measuring radiation at 11.8 μ. Triggering for synchronizing the boxcar integrator with the laser pulse is achieved by detecting a light pulse reflecting from the rotating mirror.

II. EXPERIMENTAL METHOD AND INTERPRETATION

A. Method

Consider the nonlinear cubic polarization which is responsible for the generation of a combination frequency. The polarization is given by

$$\mathfrak{P}_l{}^3(\omega_3,\mathbf{r}) = DX^4{}_{lmno}(-\omega_3,\omega_1,\omega_1,-\omega_2) \times E_m(\omega_1,\mathbf{r})E_n(\omega_1,\mathbf{r})E_o{}^*(\omega_2,\mathbf{r}), \quad (1)$$

where $\omega_3=2\omega_1-\omega_2$, $\mathbf{E}(-\omega,\mathbf{r})=\mathbf{E}^*(\omega,\mathbf{r})$, and D is a degeneracy factor which accounts for all permutations of the field components when the frequencies are not all identical. $D=3$ in this particular example. $X^4{}_{lmno}$ is an element of the fourth-rank electric susceptibility tensor. Optical difference mixing of coherent laser radiation of the form $\omega_3=2\omega_1-\omega_2$, where the two frequencies ω_1 and ω_2 are emitted by the laser and the ω_3 radiation is created by the mixing, has proven useful for studying weak nonlinear susceptibilities. This frequency combination is nearly phase-matched in the materials studied so that detectable radiation levels are achieved with susceptibilities too small to be observed by third-harmonic generation (THG) or sum-frequency mixing where the phase mismatch is a severe limitation. Maker and Terhune[1] realized the advantages of this technique and studied materials such as LiF, CaF_2, quartz, and benzene using a pulsed ruby laser and mixing the laser output with Raman stokes shifted radiation to get third-order polarizations at the antistokes frequency.

Note that materials which are not transparent to third harmonic (TH) can still be studied using difference mixing to measure the fourth-rank susceptibility tensor.

A CO_2-N_2-He laser of the type described by Patel[8] and others was operated in the Q-switched mode with mirror rotating at 200 rps, a 6-ft-long dc electrical discharge, a 1-in.-diameter plasma tube, and NaCl Brewster-angle windows. The operating pressures were $\sim$10 mm He, 1 mm air, and 1 mm CO_2, and the operating current was 25 mA. The laser output consisted of several P transitions of the 00°1-10°0 band near 10.6 μ and several P and R transitions of the 00°1-02°0 band near 9.5 μ and 9.2 μ. For the quantitative measurements, only radiation near 11.8 μ was studied, although all of the different possible frequency combinations were generated and could have been studied. Let ω_1 be the frequency of the radiation close to 10.6 μ, and ω_2 the frequency of that close to 9.5 μ. Then $\omega_3=2\omega_1-\omega_2$ is the frequency near 11.8 μ generated by difference mixing.

The experimental setup is shown in Fig. 1. The monochromator, a Spex $\frac{3}{4}$-m Czerny-Turner single-grating instrument with a 75-line/mm grating, served to identify the wavelengths and to isolate the particular frequency combination desired. Two long-pass interference filters were necessary to reduce the laser intensity transmitted to the detector below the detector noise level, since the grating scattered about 1 part in 10^5. Typical operating laser powers were 1 kW at 10.6 μ and 300 W at 9.5 μ in several lines with pulse widths of $\sim$200 nsec. A converging lens was used to create high intensities capable of generating detectable signal power levels in all crystals studied. For the materials with the smallest nonlinearities, a 10-cm-focal-length lens was used, creating a focal region characterized by a cross-sectional area of $\sim 10^{-3}$ cm^2 and a length of $\sim$3 cm. At the focus this resulted in intensities of $\sim 10^3$ kW/cm^2 at 10.6 μ and $\sim$300 kW/cm^2 at 9.5 μ. Sample thicknesses of no more than 3 mm permitted comparisons and calculations to be made under the assumption that the focused light beam did not spread appreciably in passing through the crystals.

The use of a PAR Boxcar Integrator (a gated signal-averaging device synchronized with the laser output via a trigger pulse taken off the rotating mirror) improved the signal-to-noise ratio and allowed accurate relative measurements to be made by averaging the signal over many laser pulses. The detector was a Santa Barbara Research Corp. copper-doped germanium photoconductive device, cooled to liquid-helium temperature. (See Fig. 1.)

A necessary innovation was the incorporation of a dispersive element within the laser cavity (Fig. 2). Without this dispersive element the peak power point for the higher-gain ω_1 radiation occurred $\sim$200 nsec before that for the lower-gain ω_2 radiation. Since pulses were $\sim$200 nsec long, the time overlap of the ω_1 and ω_2 radiation was very poor, so that only a small mixing signal could be generated. By giving the beams at ω_1 and ω_2 paths within the laser cavity differing by an angle equal to the angle the rotating mirror turned in

[8] C. K. N. Patel, Phys. Rev. Letters, 16, 613 (1966), and references cited therein.

200 nsec, the mode at ω_2 was made to resonate first, and its output occurred with peak power point superimposed on that of ω_1. The observed signal power at ω_3 increased by more than a hundredfold with the use of an appropriately wedged (1.2°) crystal of NaCl. (See Fig. 2.) With this arrangement detectable radiation levels at ω_3 were achieved with susceptibilities as small as 10^{-12} esu.

The experiments consisted of measuring the signal generated by focusing the laser into various samples and comparing them to one another or to a standard Ge from which the magnitude of the nonlinear susceptibility could be determined.

As explained below the signal was measured as a function of carrier concentration in n-type GaAs. To calculate χ the signal had to be corrected for linear absorption at ω_1, ω_2, and ω_3. Linear-transmission measurements were therefore made on all samples from which α, the absorption coefficient, could be calculated and applied as a correction.

Each sample of GaAs was measured via the Hall effect to determine its carrier concentration. Low-resistivity Ohmic contacts were placed on GaAs by using indium solder and baking for $\frac{1}{2}$h at 400°C in a dry-nitrogen atmosphere to cause diffusion away from the surface layer of impurities (probably copper) which created p-n junctions. The carrier concentration was calculated assuming the ratio of Hall to conductivity mobility equal to 1. Any error in this assumption will mean only a constant multiplicative factor correction to each value of n since, for the carrier concentrations and temperatures considered, the statistics were essentially Boltzmanlike with no shift in the relative occupation of energy states in the conduction band as carrier concentration was changed. Calculations of scattering mechanisms in GaAs indicate that the ratio of mobilities lies between 1 and 1.1. The maximum 10% error will be seen to be negligible compared to the inherent uncertainty in the absolute magnitude of χ which amounts to 50%.[4]

B. Interpretation

All crystals studied are of point group $m3m$ or $\bar{4}3m$ for which spatial symmetry imposes identical restrictions on the form of the fourth-rank electric susceptibility tensor.[9] The 21 nonvanishing tensor elements of $\chi_{lmno}{}^4(-\omega_3, \omega_1, \omega_1, -\omega_2)$ in general reduce to four independent components in these point groups. In the region of frequencies far from any system resonances, dispersion is negligible and the number of independent variables is further reduced to two, c_{1111} and c_{1122}.[10]

[9] P. N. Butcher, Nonlinear Optical Phenomena, Bulletin No. 200, Engineering Experiment Stations, Ohio State University, Columbus, Ohio, 1965 (unpublished) p. 47.

[10] $c_{1111}=\chi_{xxxx}=\chi_{yyyy}=\chi_{zzzz}$

$c_{1122}=\chi_{xxyy}=\chi_{yyxx}=\chi_{xyxy}=\chi_{yxyx}=\chi_{xyyx}=\chi_{yxxy}=\chi_{yyzz}=\chi_{zzyy}$
$=\chi_{yzyz}=\chi_{zyzy}=\chi_{yzzy}=\chi_{zyyz}=\chi_{zzxx}=\chi_{xxzz}=\chi_{xzxz}=\chi_{zxzx}$
$=\chi_{zxxz}=\chi_{xzzx}$.

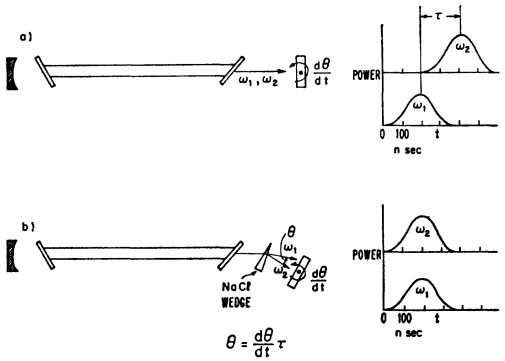

FIG. 2. a) Without dispersive NaCl wedge, ω_1 and ω_2 radiation achieve threshold at different times. Higher-gain ω_1 pulse peaks $\tau=\sim$200 nsec before ω_2. b) With wedge cut so that $(d\theta/dt)\tau=\theta, \omega_2$ starts to build up before ω_1, compensating for lower gain at ω_2. Peak-power points of ω_1 and ω_2 are now superimposed.

For a laser operating in the fundamental transverse Gaussian modes for both ω_1 and ω_2, the electric fields in the near field approximation are given by

$$\mathbf{E}(\omega_i,r,z)=\mathbf{A}_{i0}e^{-r^2/w_i^2}e^{i(k_iz-\omega_it)}e^{-(\alpha_i/2)z}, \quad i=1,2, \qquad (2)$$

where w_i is the beam spot size,[11] k_i the propagation constant, and α_i the power absorption coefficient. With ω_1 and ω_2 radiation both linearly polarized along the same cubic fourfold axis [100], (1) and (2) yield a combination frequency polarization along the same direction,

$$\mathfrak{P}(\omega_3,r,z)=3c_{1111}A_{10}{}^2A_{20}e^{-r^2/\bar{w}_3^2}e^{i[(2k_1-k_2)z-\omega_3t]} \times e^{-[\alpha_1+(\alpha_2/2)]z}, \qquad (3)$$

where $1/\bar{w}_3{}^2=2/w_1{}^2+1/w_2{}^2$.

The wave equation for $\mathbf{E}(\omega_3,r,z)$,

$$\nabla\times\nabla\times\mathbf{E}(\omega_3,r,z)+\frac{\epsilon_3\partial^2}{c^2\partial t^2}\mathbf{E}(\omega_3,r,z)=\frac{-4\pi\partial^2}{c^2\partial t^2}\mathfrak{P}(\omega_3,r,z), \qquad (4)$$

with ϵ_3 the dielectric constant and

$$\mathbf{E}(\omega_3,r,z)=\mathbf{A}_{30}(r,z)e^{i(k_3z-\omega_3t)}e^{-(\alpha_3/2)z}, \qquad (5)$$

reduces to[12]

$$\frac{\partial A_{30}(r,z)}{\partial z}=i\frac{2\pi\omega_3}{n_3c}\mathfrak{P}(\omega_3,r,z)e^{-i(k_3z-\omega_3t)}e^{(\alpha_3/2)z}, \qquad (6)$$

where it is assumed that

$$\left|\frac{\partial^2A}{\partial z^2}\right|\ll\left|k_3\frac{\partial A}{\partial z}\right|.$$

n_3 is the index of refraction at ω_3. The solution with initial condition $A_{30}(r,0)=0$, when $\mathfrak{P}(\omega_3,r,z)$ is given

[11] G. D. Boyd and J. P. Gordon, Bell System Tech. J. 40, 489 (1961).

[12] J. A. Armstong, N. Bloembergen, J. Ducuing, and P. S. Pershan, Phys. Rev. 127, 1918 (1962).

by Eq. (3), is

$$A_{30}(r,z)=\frac{i2\pi\omega_3}{n_3c}3c_{1111}A_{10}^2A_{20}e^{-r^2/\bar{w}_3^2}\frac{e^{i(\Delta k)z}e^{-(\Delta\alpha)z}-1}{i\Delta k-\Delta\alpha}, \quad (7)$$

where $\Delta k=2k_1-k_2-k_3$ and $\Delta\alpha=\alpha_1+(\alpha_2/2)-(\alpha_3/2)$. For a Gaussian beam the total power is given by

$$P_i(z)=(n_icw_i^2/16)|A_{10}|^2e^{-\alpha_iz} \quad (8)$$

as can be obtained by integrating $|E(\omega_i,r,z)|^2$ over the cross section. The total power at ω_3, emerging from a crystal of length l is then

$$P_3=\frac{256\pi^2\omega_3^2P_1^2P_2}{n_1^2n_2n_3c^4}(3c_{1111})^2\frac{4\bar{w}_3^2}{w_1^4w_2^2}\times\left|\frac{e^{i(\Delta k)l}e^{-(\Delta\alpha)l}-1}{i\Delta k-\Delta\alpha}\right|^2e^{-\alpha_3l}. \quad (9)$$

Note that the confocal parameter[11] of the focused beam within the crystal is always at least ten times the crystal thickness, justifying the use of the near-field approximation. The phase anomaly associated with a focused beam is responsible for the absence of any net THG produced by an infinite medium in which the beam is symmetrically focused.[13,14] But for these thin crystals one can show that the phase anomaly of a focused Gaussian beam is unimportant in affecting third-order mixing.

The experiments give relative values of signal power for two samples. From the relative signal power one calculates relative values of χ. In comparing one crystal to another, the beams may have any mode structure as long as it is the same for each crystal. In general, the spot size factor $4\bar{w}_3^2/w_1^4w_2^2$ is replaced by an area factor $A_3/A_1^2A_2$ (A_i is the area of the beam at frequency ω_i) multiplied by an appropriate numerical factor. Upon refracting into a crystal at the beam waist (or focal point) the area will not change so that this factor is constant from one crystal to the next, independent of an index of refraction change, and may be ignored in the comparison.

In comparing experimental signals, account must be taken of reflection from the faces of the crystal. Assuming that signal at ω_3 is generated only on the first pass through the crystal (which is slightly wedged and tilted away from normal incidence or antireflection coated to avoid coherent interference multiple reflection problems), reflectivities R_i result in a corrected formula

$$P_3=K\frac{(1-R_1)^2(1-R_2)}{(1+R_3)n_1^2n_2n_3}(c_{1111})^2\times\left|\frac{e^{i(\Delta k)l}e^{-(\Delta\alpha)l}-1}{i\Delta k-\Delta\alpha}\right|^2e^{-\alpha_3l}, \quad (10)$$

where P_3 is the transmitted total signal power and K is a proportionality constant.

For the case of arbitrary crystal orientation relative to the laser polarizations, c_{1111} is replaced by the appropriate factor derived from Eq. (1). In particular, for the laser beams incident along [100] with polarizations parallel and linearly polarized at an angle θ to [010]

$$\begin{aligned}\mathbf{E}_L(\omega_1)&=E_0(\omega_1)(\hat{x}\cos\theta+\hat{y}\sin\theta),\\ \mathbf{E}_L(\omega_2)&=E_0(\omega_2)(\hat{x}\cos\theta+\hat{y}\sin\theta).\end{aligned} \quad (11)$$

Then by (1)

$$\begin{aligned}\mathfrak{P}_x(\omega_3)&=3E_0^2(\omega_1)E_0^*(\omega_2)(c_{1111}\cos^3\theta+3c_{1122}\cos\theta\sin^2\theta),\\ \mathfrak{P}_y(\omega_3)&=3E_0^2(\omega_1)E_0^*(\omega_2)(c_{1111}\sin^3\theta+3c_{1122}\sin\theta\cos^2\theta).\end{aligned} \quad (12)$$

The polarization and radiated field at ω_3 will also be linearly polarized but, in general, they will not remain parallel to the incident beam polarizations. The total power at ω_3 will be proportional to

$$\mathfrak{P}_x^2(\omega_3)+\mathfrak{P}_y^2(\omega_3)=[3E_0^2(\omega_1)E_0^*(\omega_2)]\times[c_{1111}^2(\cos^6\theta+\sin^6\theta)+(9c_{1122}^2+6c_{1111}c_{1122})\cos^2\theta\sin^2\theta]. \quad (13)$$

Then c_{1111}^2 in Eq. (10) is replaced by

$$c_{1111}^2(\cos^6\theta+\sin^6\theta)+[9c_{1122}^2+6c_{1111}c_{1122}]\cos^2\theta\sin^2\theta. \quad (14)$$

Measurements of signal as a function of θ give only the ratio,

$$(9c_{1122}^2+6c_{1111}c_{1122})/c_{1111}^2=9(c_{1122}/c_{1111})^2+6(c_{1122}/c_{1111}). \quad (15)$$

c_{1122}/c_{1111} is then obtained as the solution of a quadratic equation with ambiguity in both sign and magnitude. If a different propagation direction is selected, independent quadratic solutions may be obtained which yield c_{1122}/c_{1111} unambiguously.

In the experiments one propagation direction [1$\bar{1}$0] and 3 orientations are sufficient. These correspond to the laser polarized along [001], [110], and [111], respectively. The ratios of signal power for the laser polarized along [110] and [111] to that given by Eq. (10) are

$$\begin{aligned}R(110/100)&=\tfrac{1}{4}(1+3c_{1122}/c_{1111})^2,\\ R(111/100)&=\tfrac{1}{9}(1+6c_{1122}/c_{1111})^2.\end{aligned} \quad (16)$$

For isotropic materials $R(110/100)=R(111/100)=1$ and $c_{1122}/c_{1111}=\frac{1}{3}$.

The relative signs of nonlinearities in two samples may be determined by a method first used by Chang *et al.*[15] and more recently by Simon and Bloembergen.[16]

[13] W. G. Rado, Appl. Phys. Letters **11**, 123 (1967).
[14] G. H. C. New and J. F. Ward, Phys. Rev. Letters **19**, 556 (1967).
[15] R. K. Chang, J. Ducuing, and N. Bloembergen, Phys. Rev. Letters, **15**, 6 (1965).
[16] H. J. Simon and N. Bloembergen, Phys. Rev. **171**, 1104 (1968).

This method utilizes the fact that a definite phase relationship exists between the electric field at ω_3 created by two or more successive plane parallel slabs of nonlinear material. This is true because of the definite phase relationship between the fields at ω_3 and the electric fields at ω_1 and ω_2 which create the nonlinear polarization through χ. By keeping track of the orientations of the crystals and therefore of the components of χ which contribute, one can predict how the electric fields at ω_3 created in successive media will interfere. In previous work this task was complicated by the need to distinguish between a + and − direction in a crystal which lacked a center of inversion, because the susceptibility tensor studied was a third-rank tensor nonlinearity, responsible for second-harmonic generation (SHG). In addition, the coherence lengths of the materials studies were relatively short, of the order of several microns, complicating the phase relationship between the SH and laser electric fields.

Here, both complications are absent. The fourth-rank susceptibility tensor does not change sign upon inversion so there is no need to distinguish between the + and − directions. Also the coherence lengths are so long that thin crystal plates can be used which are essentially phase matched, allowing the phase differences between fields at ω_1, ω_2, and ω_3 to remain essentially constant, and greatly simplifying the analysis.

Consider a plane parallel slab of nonlinear material and ignore reflection losses from the air crystal interfaces. Incident radiation at ω_1 and ω_2 creates a polarization which radiates at ω_3 with the resultant field growing linearly with the length of the crystal. If the slab is split into two pieces of equal thickness, each half generates half as much field at ω_3 as the undivided slab. The two fields are in phase and add linearly to give the same total field. If, however, the second piece should have its χ change sign, the field generated by it would be 180° out of phase with the field generated by the first piece. Since amplitudes would be equal and opposite, there would be complete destructive interference and no net radiation at ω_3. By a simple extension of the analysis, with two slabs made of different material one can determine the sign of χ in one relative to the other. Even if one slab generates a field of different amplitude than the other it is still possible to determine relative sign. For example, if slabs A and B generate amplitudes E_A and E_B, respectively, A and B in series generate total amplitude $E_A \pm E_B$, the sign being + for χ's of the same sign and − for χ's of opposite sign. The signal power goes as $(E_A \pm E_B)^2$ so that even if $|E_A| = 10|E_B|$ the signal will be 25% larger for the positive sign compared to the negative sign.

The crystals studied have large indices of refraction with reflectivities as great as 36%. To avoid the complication of having to account for reflection losses, there are two alternatives. The crystals can be antireflection coated with a coating of thickness and dispersion small enough so that the phase difference introduced may be ignored. Or using a sharply focused laser beam, both crystals can be placed in the light path. Away from the sharp focus, reflectivity losses are the same since reflectivity does not depend on intensity. Negligible mixing signal is generated in the first crystal if it is out of focus, in a region where the laser intensity is low. As this first crystal is moved into the focal plane near the second crystal the amount of mixing signal changes without a change in the transmitted laser power available to the second crystal.[17] In this way the influence of reflection losses is experimentally eliminated.

This discussion is applicable without additional considerations only when χ is real as it will be for the crystals studied in these experiments. When photon energies are comparable to or greater than bandgaps, the χ's become complex and further analysis is necessary. Chang *et al.*[15] consider this problem in detail.

III. DISCUSSION AND RESULTS

A. Valence-Electron Contribution χ^b

Theory

JB have calculated χ^b for GaAs using tetrahedral-bonding orbitals pointing in the ⟨111⟩ directions. Their definition of χ is a factor of 4 larger than that used here. Defining a component $c_{\xi\xi\xi\xi}$, where ξ is the [111] direction, their calculation give $c_{\xi\xi\xi\xi}$ (GaAs) $= -0.13\times10^{-10}$ esu. WP and JB expect one-band calculations to give accurate results for the conduction-electron contribution χ^n in GaAs, where the conditions that all photon energies are small compared to the band gap are satisfied. As will be shown in the next section on χ^n, for high resistivity GaAs, χ^n is negligible compared to χ^b.

The tetrahedral-bonding orbitals used by JB are essentially an isotropic model. WB showed that Ge and Si were anisotropic, and in general, the anisotropy is not surprising. It may, in principle, be traced to the anisotropy of the electronic band structure. Theoretical refinement of the tetrahedral-bonding orbital model might be able to take anisotropy into account by taking more realistic and accurate wave functions.

Results

Under certain conditions GaAs of the semi-insulating type can be formed by doping with oxygen. A sample with measured resistivity $\rho \cong 1.7\times10^5$ Ω cm was used to measure χ^b. Samples of this type have mobilities greater than 4000 cm²/V sec so that n is less than 10^{10}/cc, assuring that χ^n may be ignored. In this GaAs sample $|c_{1111}|$ was measured relative to Ge and the sample was shown to be anisotropic. The results are collected in Table I along with results for Ge and Si reported by WB. No change was observed by cooling

[17] The parametric assumption, that the laser power depletion due to mixing-signal generation is negligible, is made throughout this analysis.

TABLE I. Valence-Electron contribution χ^b.

	Ge	Si	GaAs (high ρ)
$\lvert c_{1111}\rvert$ (exp)	1×10^{-10} esu $\pm50\%$	$0.06\lvert c_{1111}\rvert$ (Ge) $\pm10\%$	$0.12\lvert c_{1111}\rvert$ (Ge) $\pm10\%$
$\lvert c\rvert$ (estimate)[a]	0.7×10^{-10} esu	$0.2\lvert c\rvert$ (Ge)	$0.15\lvert c\rvert$ (Ge)
c_{1122}/c_{1111}	$+0.61\pm0.02$	$+0.48\pm0.03$	$+0.25\pm0.01$
$\lvert c_{\xi\xi\xi\xi}\rvert$ (exp)[b]	1.5×10^{-10} esu $\pm50\%$	0.08×10^{-10} esu $\pm50\%$	0.10×10^{-10} esu $\pm50\%$
$c_{\xi\xi\xi\xi}$(JB)	-0.88×10^{-10} esu	-0.063×10^{-10} esu	-0.13×10^{-10} esu
l_{coh}(calc)[c]	~1 cm	~1 cm	~1 cm

[a] Miller's phenomenological rule—see WB (Reference 4).
[b] $\lvert c_{\xi\xi\xi\xi}\rvert = [R(111/100)]^{1/2}\lvert c_{1111}\rvert$.
[c] From index of refraction data of C. D. Salzberg and J. J. Villa, J. Opt. Soc. Am. 47, 244 (1957) and dispersion data available from SHG experiments of C. K. N. Patel, Phys. Rev. Letters, 16, 613 (1966).

the GaAs sample from room temperature to ~77 K°. Comparison of the Ge, Si, and GaAs data shows that the relative values are in good agreement with the theory of JB and also in reasonable agreement with an estimate based on Miller's phenomenological rule as outlined in WB.

The anisotropy is interesting. Whereas Ge and Si have the largest susceptibility for radiation polarized along ⟨111⟩, GaAs is most polarizable along ⟨100⟩. A detailed calculation aimed at explaining the difference between Ge and Si on the one hand, and GaAs on the other would probably require a full summation of electric dipole moment matrix elements over electronic $\mathbf{k}$ states with explicit account taken of the anisotropy of the electronic band structure. The agreement in magnitude for all three materials with the JB model is encouraging, anisotropy notwithstanding.

The relative signs of χ^b in Ge and GaAs were experimentally found to be the same in agreement with the JB model. However, χ^b should have the opposite sign from χ^n for this particular combination of difference mixing. This is *not* the case, as will be shown below.

B. Conduction-Electron Contribution χ^n

Theory

By studying the behavior of χ as a function of n in GaAs more can be learned about anisotropy, band structure, and even the absolute sign of χ^n. From JB in a one-band model χ^n can be calculated as

$$\chi^n{}_{xxxx}=\frac{e^4}{24\hbar^4\omega_3\omega_1{}^2(-\omega_2)}\frac{1}{V}\sum_{\mathbf{k}} f_0(E_{\mathbf{k}})\frac{\partial^4 E_{\mathbf{k}}}{\partial k_x{}^4}, \quad (17)$$

where $E_{\mathbf{k}}$ is the energy of an electron in the state $\mathbf{k}$ in the conduction band, f_0 is the Fermi function, and the sum is over the conduction band. If the surfaces of constant energy are spherical in k space near the conduction-band minimum at $k=0$, and if the conduction electrons are all sufficiently close to this minimum, χ^n is expected to be isotropic.

The magnitude of χ provides information about the dependence of $E_{\mathbf{k}}$ on $\mathbf{k}$. In particular, expanding $E_{\mathbf{k}}$ in a power series in $\mathbf{k}$, Eq. (17) implies that only terms in k^4 and higher contribute to χ^n. This affords a direct experimental means of measuring the nonparabolicity of a band, independent of the parabolic k^2 terms. Measurements such as optical transmission, reflectivity, and Faraday rotation are indirect in that the nonparabolicity is only a small correction to the parabolic behavior of the band.

The sign of χ^n is seen to depend on the sign of the nonparabolicity. For Kane's model used by WP and JB to calculate χ^n in InAs and InSb,

$$E_k=\frac{E_G}{2}\left[\left(1+\frac{2\hbar^2k^2}{m^*E_G}\right)^{1/2}-1\right]. \quad (18)$$

$\Sigma_{\mathbf{k}} f_0(E)(\partial^4E_{\mathbf{k}}/\partial k_x{}^4)$ is seen to be negative for the carrier concentrations and temperature of experimental interest (Patel *et al.*[2]) and therefore Eq. (17) predicts a positive (+) sign for χ^n. The agreement between Patel *et al.*[2] and WP for the dependence of χ on n in InAs, plus numerous other experimental investigations[18] of the conduction band structure of InAs, give strong evidence that Kane's band structure is applicable and it is safe to assume that χ^n is indeed positive for this particular frequency combination.

Applying Kane's theory to GaAs with $m^*=0.07$ m and $E_G=1.40$ eV, the one-band calculation gives $\chi^n/n\cong1.5\times10^{-27}$ esu cc so that $\chi^n\sim10^{-17}$ for $n\sim10^{10}$/cc. This assures that in the high-ρ sample of GaAs χ^n is indeed negligible compared to χ^b, a confidence borne out by measurements to be discussed.

In a given crystal of GaAs, the relative sign of χ^n and χ^b may easily be determined. For n such that $|\chi^n|=|\chi^b|$, $|\chi|=\big||\chi^b|\pm|\chi^n|\big|$ depending on the relative signs. If power at ω_3 is measured as a function of increasing n starting with $n\sim0$, the signal power will increase monotonically if the sign is positive. If the sign is negative, signal power will go through a zero when $|\chi^n|=|\chi^b|$.

Results

Figure 3 plots $|\chi|\propto\bar{S}^{1/2}$ versus $1/R\bar{\mu}$ for a sample of GaAs which at room temperature had $n\sim2\times10^{15}$/cc. The experimental point in the upper right of the Figure corresponds to room temperature. As the sample was cooled, n decreased. Experimentally, $\bar{S}^{1/2}$ was measured

[18] For example F. Stern in *Proceedings of the International Conference on Semiconductor Physics, Prague, 1960* (Academic Press Inc., New York, 1961), p. 904.

as a function of R, the sample resistance. $\bar{\mu}$ is a correction applied to account for the changing mobility of the sample.[19] $\bar{\mu}$ was not measured but extrapolated from data taken by several observers.[20] The detailed behavior of $|\chi|$ versus n is not very important. What matters is that $|\chi|$ does not go through zero. This shows that χ^b and χ^n have the same sign. For temperatures below $T=180°$K, where $1/R\bar{\mu}$ was essentially 0 on the scale of Fig. 3 and $n<10^{13}$/cc, $|\chi|$ was equal to $|\chi^b|$ measured from the high-ρ GaAs sample. This was shown by direct comparison of the high-ρ sample and the sample used for the plot in Fig. 3.

Figure 4 shows $|\chi|$ versus n for several different samples of GaAs. Each point corresponds to a different sample, and all measurements were taken at room temperature. Beams at ω_1, ω_2, and ω_3 were all polarized along the [111] direction. This establishes the value for $n=0$ as $|\chi^b|=|c_{\xi\xi\xi\xi}(\text{GaAs})|=0.1\times10^{-10}$ esu. This plot confirms the conclusion from Fig. 3 that χ^b and χ^n have the same sign.

The experimental slope is $\partial\chi/\partial n=4.4\times10^{-27}$ esu cc. The absolute magnitude of $\partial\chi/\partial n$ is subject to the $\pm50\%$ uncertainty of the vertical scale. Relative values taken with respect to the high-ρ sample as a reference are accurate to $\pm10\%$ as shown by the error bars. The horizontal error bars are due to the uncertainty in the Hall measurements of n. The sample with largest n was tested for anisotropy. To within the experimental uncertainty it was isotropic indicating that the conduction band is spherical near $k=0$ over the range of occupied states. Previous experimental investigations[21] have not detected any aspheric behavior of the $k=0$ minimum of the conduction band in GaAs.

A computer calculation of $\partial\chi/\partial n$ was made using (17) and (18). Replacing the sum with an integral, (17) becomes

$$\chi^n=\frac{e^4}{\omega_1^2\omega_2\omega_3\pi^2(m^*)^2E_G}\int dk\left(\frac{\hbar^4k^6}{m^*E_G^2D^{7/2}}-\frac{\hbar^2k^4}{m^*E_GD^{5/2}}+\frac{k^2}{4D^{3/2}}\right)\left(\frac{1}{\exp[(E-E_F)/kT]+1}\right), \quad (19)$$

$$D=1+(2\hbar^2k^2/m^*E_G), \quad (20)$$

$$E=(E_G/2)(D^{1/2}-1) \quad (21)$$

with

$$n=\frac{1}{\pi^2}\int\frac{dkk^2}{e^{(E-E_F)/kT}+1}. \quad (22)$$

With $m^*=0.07m$, $E_G=1.40$ eV, and $T=300°$K, $E_F/kT<-2$ for all n considered, so that the occupation number in the conduction band looks like the Boltzman tail of the Fermi function. Hence χ^n/n is a constant independent of n, and we expect the straight line slope in Fig. 4. However the magnitude calculated is $\partial\chi/\partial n=1.05\times10^{-27}$ esu cc. This is below the range of the experimental result including uncertainty (2.2 to 6.6×10^{-27} esu cc), and means that Kane's band structure is not correct to terms in E_k higher than k^2. This

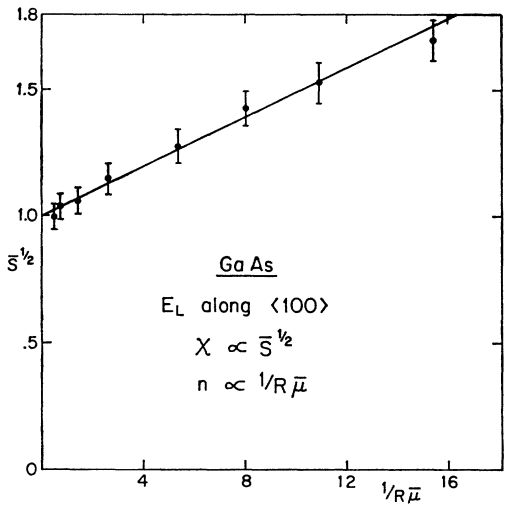

FIG. 3. Variation of (signal power)$^{1/2}$ with sample resistance in GaAs as sample temperature is changed. Signal power is normalized to 1 at its low-temperature value. The horizontal axis is conveniently normalized with dimensionless units. $\bar{\mu}$ is a relative electron mobility.

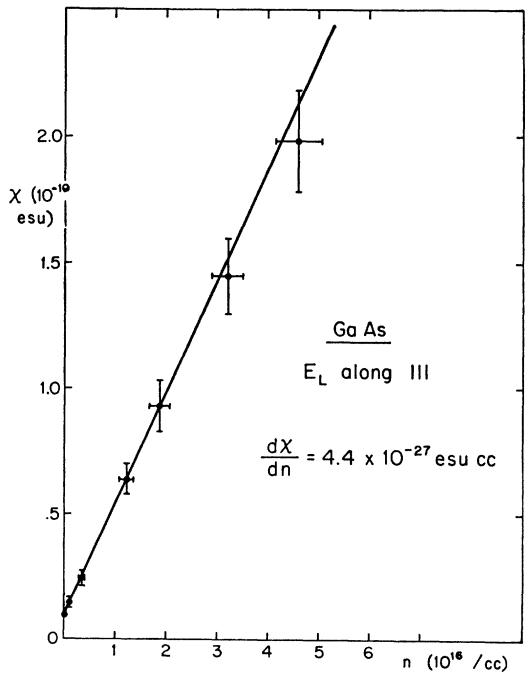

FIG. 4. Variation of nonlinear susceptibility with carrier concentration in n-type GaAs. The straight line is the fit which minimizes the fractional mean deviation from each point.

[19] Since $\sigma=ne\mu$, and $R\propto1/\sigma$, it follows that $n\propto1/R\mu$.

[20] O. Madelung, *Physics of III-V Compounds* (John Wiley & Sons, Inc., New York, 1964) p. 136.

[21] For example, H. Ehrenreich, Phys. Rev. **120**, 1951 (1960) and references cited therein.

is not surprising in GaAs inasmuch as there are known to be subsidiary conduction-band minima only ~0.3 eV above the $k=0$ minimum. Kane's model is a four-band calculation including an s-type conduction band and a p-type triplet valence band. This model is appropriate for InSb and InAs where E_G is 0.12 and 0.35 eV, respectively, and all other bands are much farther removed energetically. But in GaAs the approximations break down. The subsidiary conduction-band minima so energetically close to the $k=0$ minimum are inconsistent with Kane's model. Cardona[22] recognized this fact and his measurements provide an alternative model for the band structure. He assumes that only terms in E to k^4 need be retained. Whereas Kane's model gives

$$E\sim\frac{\hbar^2k^2}{2m^*}-\frac{\hbar^4k^4}{4(m^*)^2E_G}, \tag{23}$$

Cardona supposes that

$$E=\frac{\hbar^2k^2}{2m^*}-\frac{B\hbar^4k^4}{4(m^*)^2E_G} \tag{24}$$

is a truer representation of the band structure. The nonparabolicity is proportional to B, a dimensionless constant coefficient. By measuring reflectivity and Faraday rotation as a function of n, Cardona measures a quantity called $m_{\rm opt}$*, the reflectivity effective mass. His measurements of $m_{\rm opt}$*, differ from the result predicted by (23). In fact it is easy to show that his results are consistent with $B=2$. The nonparabolicity is roughly twice as great as predicted by Kane's model. Using (24) with $B=2$, (14), and (17), $\partial\chi/\partial n=2.94\times10^{-27}$ esu cc. This falls within the experimental uncertainty of Fig. 4. Working backwards the experimental slope gives $B=3.0\pm1.5$.

C. Relative Signs of χ

With the method of interference χ(GaAs), χ(InAs) and χ(Ge) were compared using a sample of InAs with $n=2.6\times10^{16}$/cc, GaAs with $n=1.85\times10^{16}$/cc, and Ge with $\rho\sim40$ Ω cm. In InAs, JB estimate $|c_{\xi\xi\xi\xi}|=1.5\times10^{-10}$ esu for the valence-electron contribution.

It has proven impossible to prepare crystals of InAs with $n<2\times10^{16}$/cc at which concentration χ^n is calculated to be $\sim1.5\times10^{-9}$ esu or roughly ten times the valence-electron contribution. Since the impurities responsible for this extrinsic carrier concentration do not freeze out, it is experimentally impossible to separate χ^b from χ^n in InAs and determine their relative sign as was done in GaAs. WP ignore the contribution of χ^b in InAs and the agreement of their theory with the results of Patel *et al.*[2] show that χ^b is experimentally unimportant for available crystals of InAs.

Since the nonlinearity in InAs is primarily due to conduction electrons and since no direct experimental determination of the sign of this nonlinearity is possible at these optical frequencies, the sign of χ(InAs) will be taken as positive as explained in the earlier discussion.

The InAs sample (0.6-mm thick) by itself generated 75 times as much signal as the Ge (1.15-mm thick). The Ge was antireflection-coated, but the coatings were not very good, and when Ge was inserted (out of the focal plane) in the beam in front of InAs, the signal from InAs dropped by 20%. This was consistent with the measured linear transmission of the Ge sample. When the Ge was moved into the focal plane right next to the InAs, the signal increased by 25%. These results are consistent only with the interpretation that χ(InAs) and χ(Ge) have the same sign.

Similarly AR coated Ge and GaAs each gave roughly equal signal power. A piece of GaAs followed by Ge or vice versa gave roughly four times more power than did one piece of either material alone. Also two pieces of Ge or two pieces of GaAs gave four times as much power as one piece. Again the interpretation is that χ(Ge) and χ(GaAs) have the same sign. Combining results, all three materials had the same sign for χ.

IV. CONCLUSION

The contribution to the nonlinearity in Ge is from valence electrons only. Then χ(Ge)$=\chi^b$(Ge). As has been explained χ(InAs)$\cong\chi^n$(InAs). In GaAs, χ^b and χ^n have been shown to have the same sign. Putting all this together, χ^b(Ge), χ^b(GaAs), χ^n(GaAs), and χ^n(InAs) all have the *same sign*, which is *positive*.

JB calculate a negative sign for χ^b in Ge and GaAs in contrast to the experimental results. A more elaborate orbital calculation due to Flytzanis[23] appears to give a positive sign in agreement with experiment.

The calculations have been carried out in the low-frequency approximation of photon energies less than the band-gap energy. χ^b should be frequency independent as long as this condition is met. But JB show that $\chi^n(-\omega_4,\omega_1,\omega_2,\omega_3)$ should vary as

$$\chi^n\propto1/(\omega_1\omega_2\omega_3\omega_4). \tag{25}$$

For the case of THG or the sum of three different frequencies, all frequencies in Eq. (25) are positive, and with the same nonparabolic contributing conduction band structure χ^n(GaAs) should be negative, in contrast to difference mixing where one frequency is negative. Then for THG one expects a zero in χ for a carrier concentration such that $\chi^n=-\chi^b$. Such a zero might be experimentally observable using a detector such as photovoltaic InSb which peaks in detectability near the TH at 3.53 μ. The THG signal power will be limited by a short coherence length of ~40 μ in GaAs.

[22] Manuel Cardona, Phys. Rev. **121**, 752 (1961).

[23] C. Flytzanis and J. Ducuing, Phys. Letters **26A**, 315 (1968); C. Flytzanis and J. Ducuing, Compt. Rend **266**, 344 (1968). These papers discuss calculations of the third-rank nonlinear susceptibility in III-V compounds. Unpublished work by C. Flytzanis on the fourth-rank tensor was communicated privately to Professor N. Bloembergen.

Kaw[24] has recently proposed an alternative mechanism for producing nonlinear mixing. It depends on the modulation of an energy-dependent relaxation time. His calculation is not entirely correct. The conclusion that such a mechanism is as important as the nonparabolicity in producing optical difference mixing third order in electric field is very doubtful. In particular, a correct consideration of the duration of an electron-scattering collision in GaAs shows that Kaw's mechanism would be unimportant compared to the effect of nonparabolicity.

[24] Predhiman Kaw, Phys. Rev. Letters 21, 539 (1968).

ACKNOWLEDGMENTS

The author is indebted to Dr. S. S. Jha for many stimulating discussions and useful suggestions. He thanks Professor N. Bloembergen for encouragement, helpful discussions, and for critically reading the manuscript and suggesting many useful improvements. He also acknowledges the invaluable collaboration of Dr. G. D. Boyd in the early phases of this research.

PHYSICAL REVIEW VOLUME 178, NUMBER 3 15 FEBRUARY 1969

Phonon Instability in a Magnetic Field

Y. C. LEE

Statistical Physics Laboratory, Department of Physics and Astronomy, State University of New York, Buffalo, New York 14214

AND

N. TZOAR

Department of Physics, The City College, New York, New York 10031

(Received 3 September 1968)

The problem of phonon instability of an electron-phonon system is studied. When the electrons have a net drift velocity relative to the lattice in the presence of a static, uniform magnetic field, it is found that the phonons may become unstable when certain threshold values for the drift velocity and the magnetic field are exceeded. This is more or less expected. However, even after the thresholds are exceeded, it is predicted here that there exist alternate bands of the magnetic field in which the phonons are unstable in one band, stable in the next band, unstable again in the following band, etc. These alternate bands have their origin in the discreteness of the Landau levels of the electron.

I. INTRODUCTION

RECENTLY, microwave emission from InSb was observed at various temperatures when a sample was subjected to the combined influence of dc magnetic and electric fields, provided the field strengths exceeded certain threshold values.[1–3] The physical origin of such microwave emission is not entirely clear at present. It has been suggested[4] that an instability of phonons which are first excited by the drifting electrons, with the resulting unstable longitudinal wave then coupled to an electromagnetic wave at the boundary of the sample, may possibly give rise to such radiation. This possibility has motivated us to study in more detail the problem of phonon instability of an electron-phonon system. In this system the electrons have a net dirft velocity v_D relative to the ion lattice and we assume that the system is also under the influence of a static, uniform magnetic field B_0. Although this mechanism may or may not be truly responsible for the experimentally observed radiations, the problem of phonon instability is itself of sufficient interest for an independent investigation, particularly in the low-temperature regions. Indeed, we shall find that, at temperatures $k_BT \ll \mu$, $\hbar\omega_c$, where μ and ω_c denote the Fermi energy and the electron cyclotron frequency, respectively, the phonons may become alternately unstable and stable as the magnetic field strength is varied, i.e., there exist bands of the magnetic field in which the phonons are unstable in one band, stable in the next band, unstable again in the following band, etc.

In Sec. II, a kinetic equation based on the linear approximation is set up for the phonon distribution function. This equation is then utlilzed to establish the criteria for the onset of the phonon instability in Sec. III. The growth rate of the phonon distribution function at low temperatures, which is of particular interest, is then derived and discussed in Sec. IV. A brief summary and conclusion is given in Sec. V.

[1] R. D. Larrabee and W. A. Hicinbothan, in *Proceedings of the Symposium on Plasma Effects in Solids, Paris, 1964* (Dunod Cie, Paris, 1965), Vol. 2, p. 181.

[2] S. J. Buchsbaum, A. G. Chynoweth, and W. L. Feldmann, Appl. Phys. Letters 6, 67 (1965).

[3] D. K. Ferry, R. W. Young, and A. A. Dougal, J. Appl. Phys. 36, 3684 (1965); T. Musha, F. Lindvall, and J. Hagglund, Appl. Phys. Letters 8, 157 (1966); J. C. Eidson and G. S. Kino, *ibid.* 8, 183 (1966).

[4] G. Bekefi, A. Bers, and S. R. J. Brueck, Phys. Rev. Letters 19, 24 (1967).